



Experiment Study of Effect of Apex Angle of Taper Round Tube Under Quasi Static Axial Crushing on Energy Absorption

Ze Feng Ching^(✉) and Alif Zulfakar Pokaad^(✉)

Faculty of Engineering and Technology, Multimedia University Melaka, Jalan Ayer Keroh
Lama, 75450 Bukit Beruang, Melaka, Malaysia

1181301957@student.mmu.edu.my, alif.pokaad@mmu.edu.my

Abstract. Glass Fibre Reinforced Polymer (GFRP) has gained much attraction due to their outstanding physical and mechanical properties and it is widely used for various industry. The main objective of this present studies is to investigate the change of angle in taper round tube onto its energy absorption and to analyze the performance of taper round tube in energy absorption, crushing characteristics and its crashworthiness. Besides that, crushing characteristics of GFRP taper round tubes with different angles which are 0° , 2° , 4° , 6° , and 8° was determined using Universal Testing Machine (UTM) Instron series 3367. The energy absorption was calculated from the graph which is also the area under the load-displacement curve. Furthermore, the specific energy absorption was calculated by substituting the mass of the specimen into the specific equation ($SEA = EA/mass$). To find out the effect of crashworthiness of GFRP taper round tube, the crushing process and results were recorded as well. The highest energy absorption (EA) and specific energy absorption (SEA) were 506.812 kJ and 16.999.71 kJ/kg respectively. Lastly, the relationships between each parameter are discussed in the report. The design of the specimen and fabrication preparation plays a very significant role in quasi-static axial crushing test which must be decide carefully. From this experimental study, Glass Fibre Reinforced Polymer (GFRP) taper round tube with an angle of 6° is found to be the best for energy absorber as it has the highest energy absorption and specific energy absorption (SEA).

Keywords: crashworthiness · glass fibre · epoxy resin · taper angle

1 Introduction

Axial crushing of a fibre reinforced composite tubes has been studied through massive majority of researcher [1]. Fibre reinforced round tubes have attracted much attention in many application fields such as the vehicle, aerospace & military, automotive industry, architecture, and construction [2]. Material such as aluminium, metal or fibre reinforced polymer which gain more intention in human choice, can used to fabricate the energy absorber too [3, 4]. However, because of excessive fee of material, production and renovation for metals and heavier sacrificial structure, those sorts of systems had been

discovered insufficient [5, 6]. With that, this experiment study will be carried out by using the Glass Fibre Reinforced Polymer (GFRP) material that moulded with a taper round tube that will undergoes quasi static axial crushing test.

During an impact between vehicles, the vehicle wellbeing confine secures inhabitants by keeping up with endurance space and dispersing crash powers that generally the tenants would be presented to. Crashworthiness safety system helps to prevent serious injuries from occupant during an accident but not prevent accident from happening [7]. Subsequently, a crashworthy configuration has turned into the fundamental wellbeing models of the inhabitants conveying vehicles such as vehicles, aviation and so on [8, 9]. The factor, for example, shape and thickness, fibre orientation and type of fibre material will influence the energy absorption capability. Different material will cause different results in their crushing characteristics and its crashworthiness in energy absorption [10, 11]. For example, composite material such as carbon fibre, glass fibre, fibre reinforced polymer that is subjected to axial crushing will cause of fracture whereas metallic components will undergo plastic deformation [12].

Fibre-reinforced composites have been searching tremendously in their crashworthiness application by scientist because of their low densities, stiffness, great strength, and excellent energy absorption performance therefore it is widely applied in aerospace & defense, automotive industry, wind turbine, sporting goods, and others around the world. The combination of two or more potential materials like matrix and reinforcement composite materials with much preferred mechanical performance than the matrix and reinforcement materials standing alone itself. Fibre-reinforced polymer composite offers uncovers extraordinary properties such as high strength, great performances, corrosion resistant as well as long lasting. Alternatively, in phrases of unique energy absorption and weight loss polymer composite substances are relatively brought to enhance structural energy absorption skills in addition to similarly weight reduction.

Recent years, many researchers, scholars, and scientists have reported the study of energy absorption characteristic of fibre reinforced polymer (FRP) influence by many factors such as the fibre orientation, shape and thickness, and type of fibre material. Luo et al. 2021 [13] reported that glass fibre tubes with fibre angle of 30° have the highest mean load and specific energy absorption whereas fibre angle with 45° have lowest energy absorption capability. On the other hand, Sun et al. 2018 [4] examined the crushing behaviour of filament wound CFRP composites tubes. They found that Carbon Fibre Reinforced Polymer (CFRP) tube with winding angle of 25° have the highest SEA. Hong et al. 2016 [14] researched that the mean crushing force decreasing when the taper angle is increasing and when taper angles get larger and larger the energy absorption stability factor is close to 1. Yang et al. 2016 [15] stated that the crushing force is not only depends on the thickness of the fibre layer but it also dependent on the fibre orientation. Ghamarian et al. 2018 [16] found that the energy absorption capacity can increased by increasing the apical angle, the diameter, and the length of the circular tube. Zhang et al. 2020 [17] disclosed that the small change of fibre angle will give a large F_{max} whereas large angle will give a large energy absorption and crush force efficiency.

This paper focus on the study of its energy absorption of a taper round tube that moulded by Glass Fibre Reinforced Polymer (GFRP). The objective of this research is to investigate the change of angle in taper round tube onto its energy absorption and to

analyze performance of taper round tube in energy absorption, crushing characteristics and its crashworthiness.

2 Methodology

2.1 Specimen Preparation

During the experiment, a taper round tube made of GFRP was subjected to impact by a drop tower [18, 19]. The circular tubes are designed by using Autodesk Inventor Professional 2022 and after several research have been done, the best idea design of the tool has decided in order to carry out the experiment study. The material chosen is PLA material. PLA material is chosen to print out the model by using MakerBot 3D printing. Each taper round tube was set at a height at 120 mm with the base diameter of 46 mm fixed. The infill shell was set at 50% so that the PLA material can be stronger as increases of infill shell will increase its strength. Layer height was set 0.2 mm and no of shell was set at 3. The GFRP taper round tubes are then fabricated by hand lay-up process.

The hand lay-up process was obliged to manufacture the specimen, ie Glass fibre-reinforced polymer composites. The layer of wooden board was spread by a thin layer of wax as releasing agent so that the fibre doesn't stick onto it. The roller is used to flattening the surfaces, spreading the resin, and consolidating each layer and de-bulk the fibreglass into a unitized laminant. This will expunge any air bubble entrapped between the fibreglass plies. Before proceeding to the fabrication of composites, the epoxy resin was first poured onto the metal sheet and place the glass fibre on top of it. Then continue this step layer by layer until a thickness of 1 mm was built up by impregnating the glass fibres mat with the epoxy resin mixed with hardener. The advantages of hand lay-up process are low tooling cost and widely used in many industrials which can produce larger and complex items and can customize the shape that we want. The fibre composites tube was then tested by Universal Testing Machine (UTM) as shown Fig. 2. The loading speed was set at 10mm/min.

Once the fabrication process is done, the fabricated specimen will be tested under compression test by using Universal Testing Machine (UTM). The compression strength and modulus values of the fabricated part will be tested. Fibre glass tube were fabricated according to the standard test method for compression properties of polymer matrix composite materials ASTM D695. The ASTM D695 guidelines for a specimen of our specifications are 100 mm length and 46 mm in diameter.

Lastly, a Universal Testing Machine (UTM) as shown ass Fig. 2 is used to conduct the compression test for quasi-static axial crushing of composite material ASTM D695. Saved the file name as fibre glass 0-degree column. After fixing the specimen under Universal Testing Machine (UTM), the extension was balanced all. The load was balanced as well. When the load and extension were ready then the start button is clicked. Next, the pictures of each crushing stage were taken during the axial loading test. The steps were repeated for GFRP taper round tube of 2°, 4°, 6°, and 8°. Lastly, the raw data for each specimen were recorded.

Fabrication of GFRP taper round tube will be carried out with a template so that the specimen can be cut out to produce the fibre glass sample (a). Next, the fibre glass was weighted by using weighing scale (b). The epoxy and the hardener were poured

into an empty cup and weighted as well. The mixture was then stirred until the colour changed to yellowish in colour. While stirring make sure there is no air bubbles consist in it (c)–(d). The epoxy was poured onto the fibre glass slowly and a spoon was used to make the epoxy evenly dispersed (e). After curing a piece of PVC was used to wrapped together with the fibre glass (f). Besides that, Personal Protective Equipment (PPE) were used before grinding. The fabricated specimen was clamped by using a Bench Vice (g). Lastly, a grinding machine was used in cutting the specimen. After cutting the specimen, the specimen was then weight by using the precision balance (h) (Fig. 1).

2.2 Quasi Static Compression Test

Universal Testing Machine plays a very important role in the quasi-static axial crushing test as it tests the mechanical properties and analytical study of a material and gives an accurate result. There are some standard tests can be carried out by UTM: Once the fabrication process is done, the fabricated specimen will be tested under compression test by using Universal Testing Machine (UTM). The compression strength and modulus values of the fabricated part will be tested. Due to many tests offered, a table below is created for ASTM standard which suitable for the compression test. Fibre glass tube were fabricated according to the standard test method for compression properties of polymer matrix composite materials ASTM D695. The ASTM D695 guidelines for a specimen of our specifications are 100 mm length and 46 mm in diameter.

2.3 Crashworthiness Formula

2.3.1 Energy Absorption (EA)

Energy absorption can be defined as the power to absorb various forms of energy and utilize it in some way [20]. For quasi static axial crushing process, the energy absorption represented the area under the load vs displacement graph and can determined as:

$$EA = \int_0^d F ds \quad (1)$$

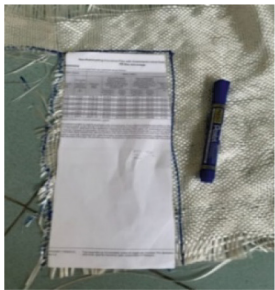
where F is the crush force in axial direction and d is the final displacement in the axial direction.

2.3.2 Specific Energy Absorption (SEA)

The specific energy absorption can be obtained from the material that is undergoes in quasi-static axial crushing of fibre reinforced composite material [21].

$$SEA = \frac{EA}{m} \quad (2)$$

where SEA is the energy absorbed per unit mass (kJ/kg), and m is the mass of the specimens (kg).



(a)



(b)



(c)



(d)



(e)



(f)



(g)



(h)

Fig. 1. Steps of hand layup technique

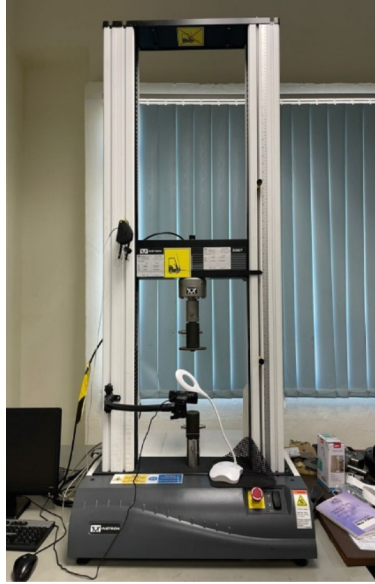


Fig. 2. Universal Testing Machine (UTM) Instron Series 3367

2.3.3 Mean Load (P_m)

Mean load is calculated by averaging the total crushing load across the full length of the deformation in the post-crushing phase.

$$F_{mean} = \frac{EA}{d} \quad (3)$$

Mean crushing load is noted as F_{mean} , the total force applied on the specimen, EA , and d represents the final crush distance.

2.3.4 Crushed Force Efficiency (CFE)

The crush force efficiency, CFE, is the parameter that can be used to determine the best energy absorbing material. It is possible to assess the performance of a specimen as a ratio of the mean load to the peak load, which is known as crush force efficiency. CFE can be mathematically formulated as follows:

$$CFE = \frac{F_{mean}}{PCF} \quad (4)$$

where CFE is the crush force efficiency, F_{mean} is the mean crushing load (kN), and PCF is the peak crushing force.

3 Results and Discussion

3.1 Results of Quasi-Static Axial Crushing Test

3.1.1 Load vs Displacement Trend Graph for 0°

Figure 3 shows the crushing trend of GFRP taper round tube with 0° . During the pre-crushing phase, the curve increases linearly until the displacement about 8.8 mm the first peak load of 5.2 kN was obtained. Then, the load value decreases tremendously to 3 kN at a displacement about 30 mm before the curve start varying during the post-crushing phase.

During the compression stage, the curve commences rising dynamically at the displacement about 75 mm which mean the load dramatically increase until the peak load reach as high as it goes. This is because the entire part of the GFRP taper round tube has been compacted at the final stage of axial loading (Fig. 4).

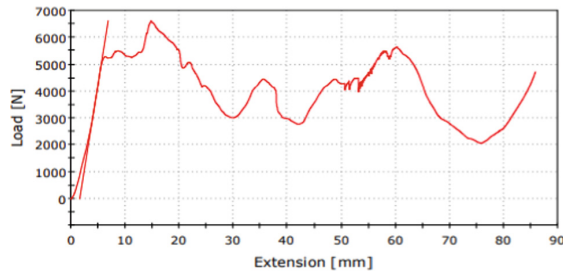


Fig. 3. Load vs extension graph of GFRP 0°

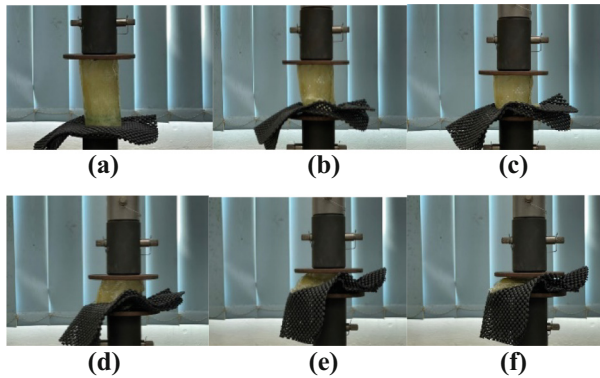


Fig. 4. Crushing phase of GFRP 0° . (a) At 0 mm displacement. (b) At 10 mm displacement. (c) At 30 mm displacement. (d) At 50 mm displacement. (e) At 70 mm displacement. (f) At 80 mm displacement.

3.1.2 Load vs Displacement Trend Graph for 2°

Figure 5 shows the crushing trend of GFRP taper round tube with 2°. As During the pre-crushing phase, the curve increases linearly until the displacement about 11 mm the first peak load of 6.9 kN was obtained. Then, the load value decreases tremendously to 2 kN at a displacement about 85 mm before the curve start varying during the post-crushing phase.

During the compression stage, the curve commences rising dynamically at the displacement about 88 mm which mean the load dramatically increase until the peak load reach as high as it goes. This is because the entire part of the GFRP taper round tube has been compacted at the final stage of axial loading (Fig. 6).

3.1.3 Load vs Displacement Trend Graph for 4°

Figure 7 shows the crushing trend of GFRP taper round tube with 4°. During the pre-crushing phase, the curve increases linearly until the displacement about 8.8 mm the first peak load of 3.1 kN was obtained. Then, the load value decreases tremendously to 1.5 kN

Table 1. Crashworthiness parameters of all the GFRP tube.

	Angle of taper round tube	Mass of the material (kg)	Energy Absorption, EA (kJ)	Specific Energy Absorption, EA (kJ/kg)	Mean Crushing Force, F_m (kN)	Crushing force efficiency, CFE
1 st Set	0°	0.04812	340.982	7,085.347	4.011	0.61
	2°	0.03585	297.071	8,284.441	3.494	0.49
	4°	0.03107	161.930	5,210.295	1.905	0.60
	6°	0.02981	506.812	16,999.706	5.962	2.15
	8°	0.02969	447.778	15,078.224	5.267	0.44
2 nd Set	0°	0.04795	349.032	7,279.082	4.106	0.69
	2°	0.03734	326.161	8,733.499	3.837	0.63
	4°	0.03049	241.934	7,933.320	2.846	0.72
	6°	0.02764	357.893	12,944.642	4.210	1.11
	8°	0.02586	325.648	12,594.663	3.831	0.36
3 rd Set	0°	0.04835	407.201	8,420.917	4.790	0.70
	2°	0.03554	415.873	11,699.587	4.892	0.48
	4°	0.03203	445.135	13,895.715	5.236	0.66
	6°	0.02935	417.909	14,234.938	4.916	0.83
	8°	0.02576	267.548	10,383.360	3.147	0.61

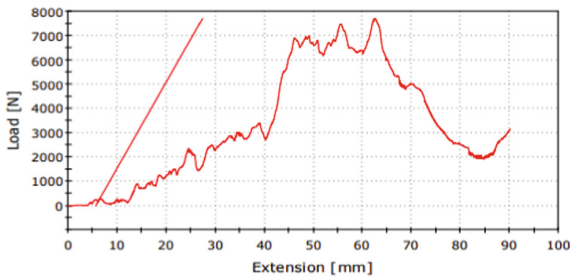


Fig. 5. Load vs extension graph of GFRP 2°

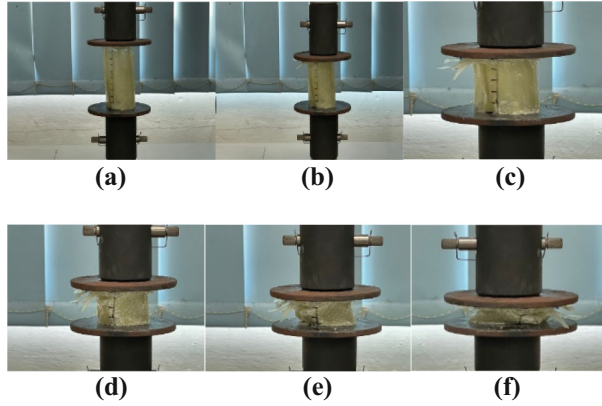


Fig. 6. Crushing phase of GFRP 2°. (a) At 0 mm displacement. (b) At 10 mm displacement. (c) At 30 mm displacement. (d) At 50 mm displacement. (e) At 70 mm displacement. (f) At 80 mm displacement.

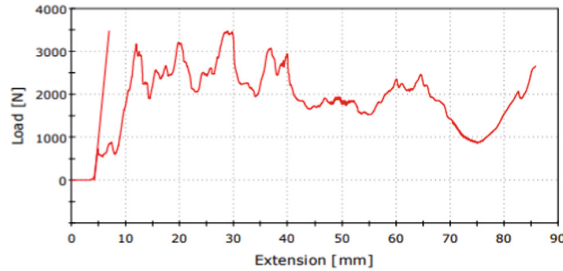


Fig. 7. Load vs extension graph of GFRP 4°

at a displacement about 55 mm before the curve start varying during the post-crushing phase.

During the compression stage, the curve commences rising dynamically at the displacement about 75 mm which mean the load dramatically increase until the peak load reach as high as it goes. This is because the entire part of the GFRP taper round tube has been compacted at the final stage of axial loading (Fig. 8).

3.1.4 Load vs Displacement Trend Graph for 6°

Figure 9 shows the crushing trend of GFRP taper round tube with 6°. During the pre-crushing phase, the curve increases linearly until the displacement about 8.8 mm the first peak load of 2.7 kN was obtained and goes to its maximum load of 10.3 kN about 25 mm. Then, the load value decreases tremendously to 4 kN at a displacement about 30 mm before the curve start varying during the post-crushing phase.

During the compression stage, the curve commences rising dynamically at the displacement about 82mm which mean the load dramatically increase until the peak load

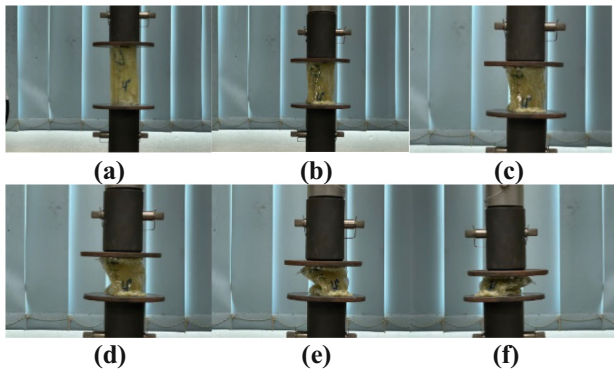


Fig. 8. Crushing phase of GFRP 4°. (a) At 0 mm displacement. (b) At 10 mm displacement. (c) At 30 mm displacement. (d) At 50 mm displacement. (e) At 70 mm displacement. (f) At 80 mm displacement.

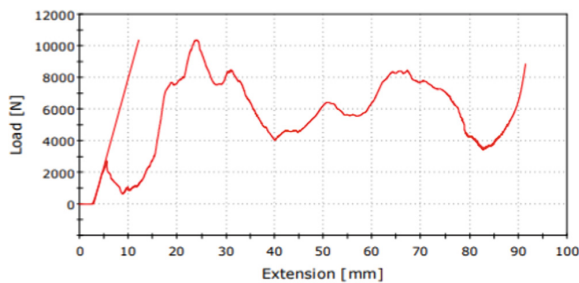


Fig. 9. Load vs extension graph of GFRP 6°

reach as high as it goes. This is because the entire part of the GFRP taper round tube has been compacted at the final stage of axial loading (Fig. 10).

3.1.5 Load vs Displacement Trend Graph for 8°

Figure 11 shows the crushing trend of GFRP taper round tube with 8°. During the pre-crushing phase, the curve increases linearly until the displacement about 24 mm the first peak load of 11.9 kN was obtained. Then, the load value decreases tremendously to 2 kN at a displacement about 35 mm before the curve start varying during the post-crushing phase.

During the compression stage, the curve commences rising dynamically at the displacement about 83 mm. Which mean the load dramatically increase until the peak load reach as high as it goes. This is because the entire part of the GFRP taper round tube has been compacted at the final stage of axial loading (Fig. 12).

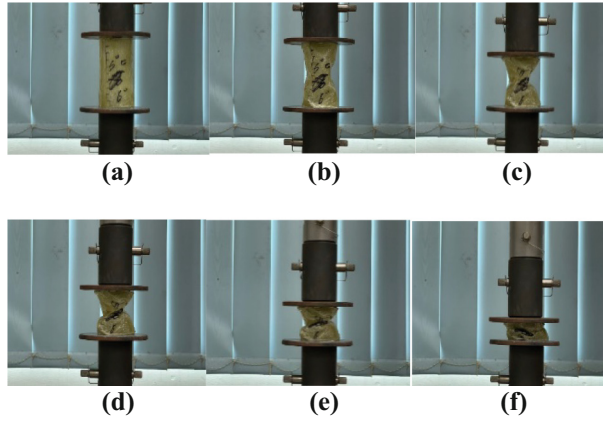


Fig. 10. Crushing phase of GFRP 6°. (a) At 0 mm displacement. (b) At 10 mm displacement. (c) At 30 mm displacement. (d) At 50 mm displacement. (e) At 70 mm displacement. (f) At 80 mm displacement.

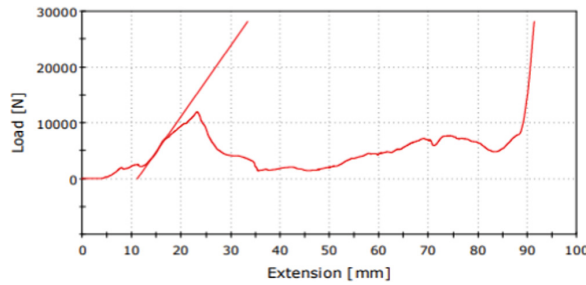


Fig. 11. Load vs extension graph of GFRP 8°

3.2 Crashworthiness Parameter

To identify the most suitable for energy absorber of composite tube structure, it is necessary to consider critical components of parameters such as energy absorption, specific energy absorption, mean crushing force, and peak load. These parameters will be discussed and compared in detail. As designated in Table 1, the crashworthiness parameters of a GFRP taper round tube with different angles.

The value of energy absorption of each taper round tube with 5 different angles (0°, 2°, 4°, 6°, and 8°) is shown in Fig. 13. Energy absorption is the ability of the material to withstand the force. When comparing the energy absorption capacities of GFRP taper round tube with various materials and masses, it is important to employ a specific energy absorption concept. In general, the greater the value of specific energy absorption, the more efficient the energy absorber are. In terms of energy absorption, GFRP with 6° obtained the highest value of 506.812 kJ. GFRP 4° attained the lowest energy absorption with the value of 161.93 kJ. Besides that, specific energy absorption can be obtained from the total energy absorption per unit mass of the specimen. To

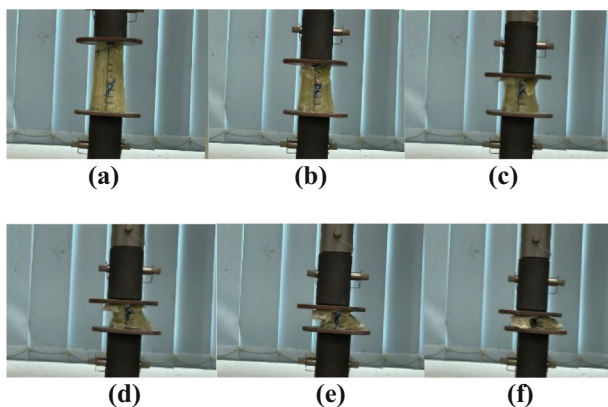


Fig. 12. Crushing phase of GFRP 8°. (a) At 0 mm displacement. (b) At 10 mm displacement. (c) At 30 mm displacement. (d) At 50 mm displacement. (e) At 70 mm displacement. (f) At 80 mm displacement.

consider a good energy absorber of the composite tube it is necessary to compare their SEA value. The greater the value of specific energy absorption, the more competent the energy absorber are. In terms of specific energy absorption, GFRP with 6° obtained the highest value of 16,999.71 kJ/kg. GFRP 4° attained the lowest energy absorption with the value of 5210.30 kJ/kg. Table 1 show that an increase of taper angle, the energy absorption and specific energy absorption will increase as well. However, the value of energy absorption decreases as the taper angle increase from 0 degree to 4 degree due to the total energy absorption are nearly identical.

3.3 Compression Results

After all the specimens subjected to a quasi-static compression test under Universal Testing Machine (UTM), the crushed GFRP taper round tube of all different angles is shown in Fig. 13. Specimens under progressive crushing will results in local buckling which is also known as loss of stability. Local buckling is a type of failure occurs in fibre reinforced composite tube that loaded in compression causing a change of deformation of the composite tube. This behaviour usually happened in ductile fibre reinforced tube or pipe columns. During this test, local buckling happened at the most of tube's top surface when the UTM cross head crushing the tube axially. For the rest of the tubes, it was found brittle fracture as there are some shattered around the tubes whereas GFRP taper round tube of 0° in Fig. 13(a) shows laminar buckling GFRP taper round tube of 6° in Fig. 13(d) shows the failure of twisting. Thus, the results of compression test causing all the specimen are resembled in a mushroom shape.

3.4 Comparison of Results

The results of quasi-axial crushing test are in line with the results in the literature review. Luo et al. [13] found that most of the tubes exhibited progressive crushing failure which

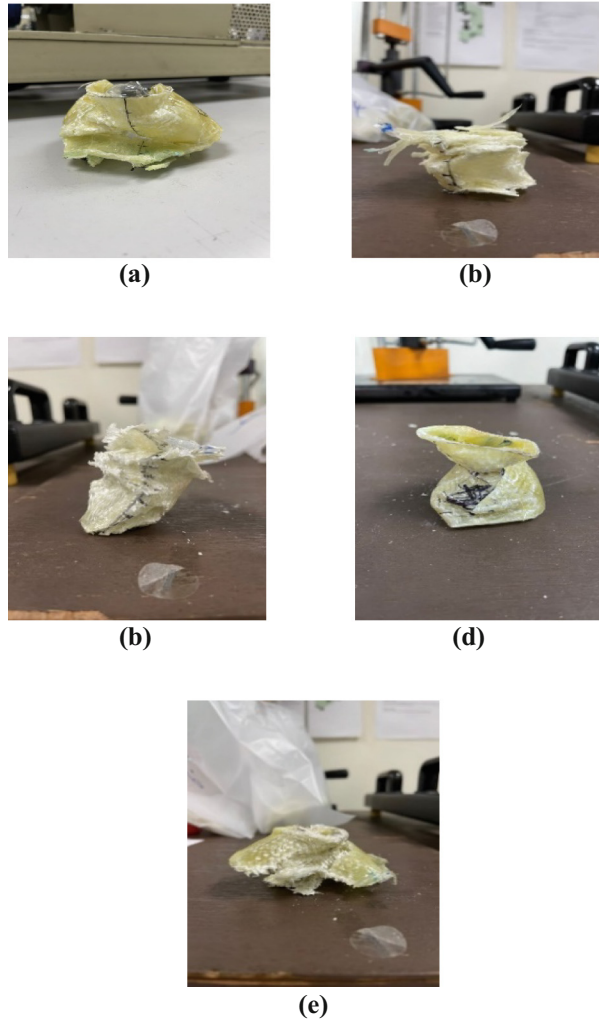


Fig. 13. Crushed specimen of GFRP. (a) GFRP 0° . (b) GFRP 2° . (c) GFRP 4° . (d) GFRP 6° . (e) GFRP 8° .

results in some of the basic failure modes. As it reported that the fibre composites tube under compression results in tear failure and transverse shear failure and form inner & outer petal delamination. The only different is the GFRP taper round tube of 6° in Fig. 13(d) shows the failure of twisting during compression whereas all the GFRP tubes occurred cracking and brittle fracture. Anyway, in Luo's article it gets the experimental results of highest SEA when the ply angle is 30° whereas lowest energy absorption when the ply angle is 45° . By comparing to the results of my current study, the increase of ply angle will increase in SEA. Based on the SEA results of my current study it is not same with Luo et al. [13]. Moreover, Sun et al. [4] reported that winding angle of 25° has the highest SEA compared to 50° , 75° , and 90° . This means that an increase of the

winding angle will decrease in the EA and SEA. It also found that when the thickness of the laminate increase, the EA and SEA will increase as well. In future study, we can also do our research on the thickness on the crashworthiness characteristics of Fibre Reinforced Composite (FRC). However, some of the results of compression test in our specimen might not be same with other research study. In a nutshell, we can conclude that the taper angle will influence on the crushing characteristics of GFRP round tube on its energy absorption.

4 Conclusion

1. In this research study, Glass Fibre Reinforced Polymer (GFRP) taper round tube were prepared and the effect of its crashworthiness under quasi-static axial crushing test were investigated.
2. The objectives to investigate the change of angle in taper round tube onto its energy absorption and to analyze the performance of taper round tube in energy absorption, crushing characteristics and its crashworthiness have been achieved successfully. The undertaken activities and key points in accomplishing these objectives are summarized as below.
3. Universal Testing Machine (UTM) Instron Series 3367 is used to obtain the maximum compression load, maximum test force, fracture value and yield value automatically. Average of energy absorption, specific energy absorption (SEA), and mean crushing force for every different angle of the taper round tube is calculated and the load-displacement graph is plotted as well. The relationship between each parameter to axial force are discussed clearly.
4. In conclusion, Glass Fibre Reinforced Polymer (GFRP) with an angle 6° has obtained the highest energy absorption and specific energy absorption (SEA). Thus, a higher specific energy absorption (SEA) value shows that the structural composite material has a higher capacity of the energy absorption.

Acknowledgments. Sincere appreciation and thank you to Faculty of Engineering and Technology, Multimedia University Melaka, for providing all the sources and equipment throughout the process of completing the research study.

References

1. H. W. Song, Z. M. Wan, Z. M. Xie, and X. W. Du, "Axial impact behavior and energy absorption efficiency of composite wrapped metal tubes," *International Journal of Impact Engineering*, vol. 24, no. 4, pp. 385–401, Apr. 2000, doi: [https://doi.org/10.1016/S0734-743X\(99\)00165-7](https://doi.org/10.1016/S0734-743X(99)00165-7).
2. A. B. M. Supian, S. M. Sapuan, M. Y. M. Zuhri, E. S. Zainudin, and H. H. Ya, "Hybrid reinforced thermoset polymer composite in energy absorption tube application: A review," *Defence Technology*, vol. 14, no. 4, pp. 291–305, Aug. 2018, doi: <https://doi.org/10.1016/J.DT.2018.04.004>.

3. A. Baroutaji, M. Sajjia, and A. G. Olabi, "On the crashworthiness performance of thin-walled energy absorbers: Recent advances and future developments," *Thin-Walled Structures*, vol. 118, pp. 137–163, Sep. 2017, doi: <https://doi.org/10.1016/J.TWS.2017.05.018>.
4. G. Sun, Z. Wang, J. Hong, K. Song, and Q. Li, "Experimental investigation of the quasi-static axial crushing behavior of filament-wound CFRP and aluminum/CFRP hybrid tubes," *Composite Structures*, vol. 194, pp. 208–225, Jun. 2018, doi: <https://doi.org/10.1016/J.COMPSTRUCT.2018.02.005>.
5. A. Rabiee, H. Ghasemnejad, A. Rabiee, and H. Ghasemnejad, "Progressive Crushing of Polymer Matrix Composite Tubular Structures: Review," *Open Journal of Composite Materials*, vol. 7, no. 1, pp. 14–48, Jan. 2017, doi: <https://doi.org/10.4236/OJCM.2017.71002>.
6. C. McGregor, R. Vaziri, A. Poursartip, and X. Xiao, "Axial crushing of triaxially braided composite tubes at quasi-static and dynamic rates," *Composite Structures*, vol. 157, pp. 197–206, Dec. 2016, doi: <https://doi.org/10.1016/J.COMPSTRUCT.2016.08.035>.
7. G. C. Jacob, J. F. Fellers, and J. M. Starbuck, "Energy Absorption in Polymer Composite Materials for Automotive Crashworthiness".
8. R. D. Hussein, D. Ruan, G. Lu, and I. Sbarski, "Axial crushing behaviour of honeycomb-filled square carbon fibre reinforced plastic (CFRP) tubes," *Composite Structures*, vol. 140, pp. 166–179, Apr. 2016, doi: <https://doi.org/10.1016/J.COMPSTRUCT.2015.12.064>.
9. W. Liu, J. Lian, S. Münstermann, C. Zeng, and X. Fang, "Prediction of crack formation in the progressive folding of square tubes during dynamic axial crushing," *International Journal of Mechanical Sciences*, vol. 176, p. 105534, Jun. 2020, doi: <https://doi.org/10.1016/J.IJMECSCI.2020.105534>.
10. D. Zhang, G. Lu, D. Ruan, and Q. Fei, "Energy absorption in the axial crushing of hierarchical circular tubes," *International Journal of Mechanical Sciences*, vol. 171, p. 105403, Apr. 2020, doi: <https://doi.org/10.1016/J.IJMECSCI.2019.105403>.
11. X. Fu, X. Zhang, and Z. Huang, "Axial crushing of Nylon and Al/Nylon hybrid tubes by FDM 3D printing," *Composite Structures*, vol. 256, p. 113055, Jan. 2021, doi: <https://doi.org/10.1016/J.COMPSTRUCT.2020.113055>.
12. S. T. W. Lau, M. R. Said, and M. Y. Yaakob, "On the effect of geometrical designs and failure modes in composite axial crushing: A literature review," *Composite Structures*, vol. 94, no. 3, pp. 803–812, Feb. 2012, doi: <https://doi.org/10.1016/J.COMPSTRUCT.2011.09.013>.
13. H. Luo, D. Zhang, Z. He, X. Li, and Z. Li, "Experimental investigation of the quasi-static and dynamic axial crushing behavior of carbon/glass epoxy hybrid composite tubes," *Materials Today Communications*, vol. 26, p. 101941, Mar. 2021, doi: <https://doi.org/10.1016/J.MTCOMM.2020.101941>.
14. W. Hong, C. Lai, and H. Fan, "Frusta structure designing to improve quasi-static axial crushing performances of triangular tubes," *International Journal of Steel Structures* 2016 16:1, vol. 16, no. 1, pp. 257–266, Mar. 2016, doi: <https://doi.org/10.1007/S13296-016-3019-7>.
15. L. W. Ying, F. P. Yang, and X. Wang, "Analytical method for the axial crushing force of fiber-reinforced tapered square metal tubes," *Composite Structures*, vol. 153, pp. 222–233, Oct. 2016, doi: <https://doi.org/10.1016/J.COMPSTRUCT.2016.05.108>.
16. A. Ghamarian and S. Azarakhsh, "Axial crushing analysis of polyurethane foam-filled combined thin-walled structures: experimental and numerical analysis," vol. 24, no. 6, pp. 632–644, Nov. 2018, doi: <https://doi.org/10.1080/13588265.2018.1506604>.
17. M. Zang, Y. Hu, J. Zhang, W. Ye, and M. Zhao, "Crashworthiness of CFRP/aluminum alloy hybrid tubes under quasi-static axial crushing," *Journal of Materials Research and Technology*, vol. 9, no. 4, pp. 7740–7753, Jul. 2020, doi: <https://doi.org/10.1016/J.JMRT.2020.05.046>.
18. C. Reuter, K. H. Sauerland, and T. Tröster, "Experimental and numerical crushing analysis of circular CFRP tubes under axial impact loading," *Composite Structures*, vol. 174, pp. 33–44, Aug. 2017, doi: <https://doi.org/10.1016/J.COMPSTRUCT.2017.04.052>.

19. S. K. Tak and M. A. Iqbal, "Axial compression behaviour of thin-walled metallic tubes under quasi-static and dynamic loading," *Thin-Walled Structures*, vol. 159, p. 107261, Feb. 2021, doi: <https://doi.org/10.1016/J.TWS.2020.107261>.
20. A. Esnaola, I. Tena, J. Aurrekoetxea, I. Gallego, and I. Ulacia, "Effect of fibre volume fraction on energy absorption capabilities of E-glass/polyester automotive crash structures," *Composites Part B: Engineering*, vol. 85, pp. 1–7, Feb. 2016, doi: <https://doi.org/10.1016/J.COMPOSITESB.2015.09.007>.
21. S. Santosa and T. Wierzbicki, "Crash behavior of box columns filled with aluminum honeycomb or foam," *Computers & Structures*, vol. 68, no. 4, pp. 343–367, Aug. 1998, doi: [https://doi.org/10.1016/S0045-7949\(98\)00067-4](https://doi.org/10.1016/S0045-7949(98)00067-4).

Open Access This chapter is licensed under the terms of the Creative Commons Attribution-NonCommercial 4.0 International License (<http://creativecommons.org/licenses/by-nc/4.0/>), which permits any noncommercial use, sharing, adaptation, distribution and reproduction in any medium or format, as long as you give appropriate credit to the original author(s) and the source, provide a link to the Creative Commons license and indicate if changes were made.

The images or other third party material in this chapter are included in the chapter's Creative Commons license, unless indicated otherwise in a credit line to the material. If material is not included in the chapter's Creative Commons license and your intended use is not permitted by statutory regulation or exceeds the permitted use, you will need to obtain permission directly from the copyright holder.

